Clim Dyn
DOI 10.1007/s00382-011-1116-z

Seasonal variations of the links between the interannual variability of South America and the South Pacific

Laura Zamboni · Fred Kucharski · C. Roberto Mechoso

Received: 12 January 2011 / Accepted: 30 May 2011

Abstract The present study focuses on the leading interannual mode of continental-scale atmospheric variability over South America, which is characterized by an equivalent barotropic vortex (referred to as VOSA in the text) centered over the eastern subtropical coast of the continent. The principal aim is to determine whether and in what season VOSA is the downstream extension of the leading Pacific South American mode (PSA1). Another objective is to examine the extent to which VOSA and PSA1 are forced by El Niño Southern Oscillation (ENSO). The research is based on examination of reanalysis data and output of experiments with an atmospheric general circulation model. The emphasis is on the southern spring, summer and fall seasons, during which VOSA modulates the interannual precipitation variability over the continent. A similar relationship is not found during the southern winter. It is found that VOSA is an integral part of PSA1 during spring and fall. In these seasons, PSA1/VOSA is originated primarily by large-scale atmospheric *internal* variability with the forcing by ENSO accounting for 14 and 8% of the total variance, respectively. During the southern summer season, when ENSO peaks, PSA1 is not a dominant mode of atmospheric variability, and VOSA primarily results from continental-scale internal variability.

Keywords PSA modes · South America · Interannual variability · ENSO teleconnections

1 Introduction

Several studies have documented a link between El Niño Southern Oscillation (ENSO) and precipitation anomalies over subtropical South America (SA) during the southern spring (Aceituno 1988; Rao and Hada 1990; Grimm et al. 1998; Montecinos et al. 2000). Similar relationships during the southern summer and fall seasons were also reported, albeit with lower significance (Silvestri 2004; Pisciottano et al. 1994; Grimm et al. 1998, 2000, 2003, 2007). The search for teleconnection mechanisms between ENSO and climate variability over SA has highlighted the importance of the leading modes of circulation variability in the South Pacific Ocean. These are the Pacific South American modes (PSA, Kidson 1988), which we next briefly review since they are of central relevance to the present study.

The PSA modes are wave-like patterns with horizontal scales of approximately zonal wavenumber three. They account for a large amount of variance of the circulation (10–20%) at the interannual timescale and have larger amplitudes in the Pacific-South American sector (Carril and Navarra 2001; Cai and Watterson 2002). Kidson (1988) obtained the structures of the two leading PSA patterns—referred to as PSA1 and PSA2 in the literature—via point correlation and Empirical Orthogonal Function (EOF) analyses. Subsequent studies found similar structures using different datasets (e.g., Mo 2000), while results at several atmospheric levels revealed the equivalent barotropic

L. Zamboni (✉)
Mathematics and Computer Science Division,
Argonne National Laboratory, 9700 S.Cass Ave TCS Bldg #240,
Argonne, IL 60439, USA
e-mail: lzamboni@mcs.anl.gov

L. Zamboni · F. Kucharski
Earth System Physics Section, Abdus Salam International Centre for Theoretical Physics, Strada Costiera 11, 34014 Trieste, Italy

L. Zamboni · C. R. Mechoso
Department of Atmospheric and Oceanic Sciences,
University of California Los Angeles, Los Angeles, CA, USA

Published online: 22 June 2011

structure of the modes (Mo and Paegle 2001; Robertson and Mechoso 2000; Mo and Higgins 1998; Kidson 1999).

Only a few studies have reported the existence of the PSA patterns at intraseasonal time scales, which required pre-filtering the data to remove longer timescales. Kidson (1999), for example, did not obtain the intraseasonal PSA patterns (10–50-day range) during either summer or winter. Ghil and Mo (1991) used an independent dataset from the one used by Kidson (1999) and tested, for the same seasons, the sensitivity of the results in three intervals of band-pass filtered data (10–90; 10–120; 10–150 days). Their findings did not include any pattern resembling the PSA modes in the first six leading EOFs of intraseasonal variability. Mo and Paegle (2001) and Mo and Higgins (1998) obtained clear signatures of the PSA modes by extracting signals at the intraseasonal scale first and performing seasonal averages next. The latter filters the intraseasonal variability, thus the result enhances signals with timescales ranging between the intraseasonal and longer. By the means of cluster analysis Cazes-Boezio et al. (2003) identified wavetrain-like regimes markedly similar to the PSA modes in spring, summer, and from fall through winter. These authors showed that changes in the amplitude and frequency of occurrence of these regimes determine their presence at the interannual timescale in spring and from fall through winter, but not in summer. Other authors have associated intraseasonal PSA patterns to Madden-Julian Oscillation (MJO) events. In our interpretation of these results, the characteristic periods of PSA modes range between the intraseasonal and the interannual timescales. In the present study we focus on the latter.

The majority of studies on the variability of the large-scale flows in the Southern Hemisphere have pooled all seasons together, the rationale being that the seasonal cycle is not large in this hemisphere (Lau et al. 1994). However, suggestions of seasonal differences have been found. For example, according to Kidson (1999), in summer the PSA modes cannot be discriminated from noise. Also for summer, Carril and Navarra (2001) identified a pattern bearing only marginal similarities with PSA1. For the winter season, Carril and Navarra (2001) found PSA1 and PSA2 as the 2nd and 3rd mode of interannual variability, and Kidson (1999) detected PSA1. Cai and Watterson (2002) reported the existence of broad similarities between PSA patterns obtained on the basis of annual and monthly anomalies at the interannual and intradecadal timescales. This variability among seasons makes results sensitive to the preprocessing made on the data, especially at the intraseasonal scale. The patterns obtained by pooling all seasons together are likely to be dominated by the circulation in spring and winter (Cai and Watterson 2002).

A large number of studies discussed the existence of associations between ENSO and the PSA modes. The link presented by Karoly (1989) was based on compositing seasonal 200 hPa height anomalies over the three ENSO events between 1972 and 1983. Corresponding to the developing phase of ENSO, in the southern winter (June through August), he identified a wave pattern at high latitudes similar to PSA1. Another view of the association between ENSO and PSA1 is presented in Mo and Paegle (2001). These authors showed that the composite of rainfall over SA during PSA1 events in summer resembles the leading EOF of rainfall, with a 0.5 correlation between the timeseries of the corresponding principal components. Furthermore, during PSA1 events, rainfall is enhanced from eastern to central Pacific and reduced to the west, consistently with the ENSO response. The strongest consensus on the existence of PSA1-ENSO links corresponds to the spring season (Garreaud and Battisti 1999; Cazes-Boezio et al. 2003; Mo and Paegle 2001). It has been suggested that ENSO amplifies or excites the PSA1 pattern without changing its structure or merely causing it (Cazes-Boezio et al. 2003; Mo and Higgins 1998 and Cai and Watterson 2002). The consensus on the existence of PSA1-ENSO links is not as strong during the southern summer, when the PSAs have weak amplitudes. Mo and Paegle (2001) argued for such a link, while Karoly (1989), Cazes-Boezio et al. (2003), Carril and Navarra (2001), and Garreaud and Battisti (1999) did not find evidence of it.

Since we are interested in rainfall over subtropical South America, our search for ENSO teleconnections must elucidate whether the PSAs are also involved and connected to the leading modes of variability over the continent. A large number of studies discuss the role of the PSA as teleconnection between ENSO and rainfall over South Eastern South America (SESA). Composites of outgoing longwave radiation anomalies (OLRA) over PSA1 events in the winter revealed enhanced convection over central-western tropical Pacific and reduced convection over the Indian Ocean (Mo and Higgins 1998). The small correlation (0.3) between Principal Components (PCs) of OLR and PSA and the lack of matching in their characteristic periods, however, indicated that the PSA modes in the interannual time scales are not simply generated as responses to variability of tropical convection.

In a recent paper, Zamboni et al. (2010) demonstrated the existence of seasonal modulations in the moisture transport from the tropics and the subtropical Atlantic toward SESA in association with the variability of an equivalent barotropic continental-scale vortex. This vortex, previously noticed by Robertson and Mechoso (2000) for the January–March period, is the leading mode of variability of 200 hPa horizontal winds over SA in October–November and in April–May, and the 2nd leading mode in January–February and June–July. In the remaining of the text we will refer to this vortex as VOSA. Some studies of

the PSA modes find a continental scale vortex resembling VOSA and interpret it as a downstream extension of PSA1 and hence an integral part of this pattern (Mo and Paegle 2001; Lau et al. 1994; Mo and Higgins 1998; Kidson 1999; Kiladis and Mo 1998). In other studies, however, this association between PSA1 and VOSA is elusive (Mo 2000; Kidson 1988; Cai and Watterson 2002; Robertson and Mechoso 2003).

The main question addressed in the present study is the existence of a relationship between VOSA and PSA1. A complementary question is the extent to which VOSA and PSA1 are forced by ENSO. The answers to these questions are of relevance to seasonal predictability since Zamboni et al. (2010) demonstrated that VOSA can be a useful predictor of precipitation over SESA. We attempt to put on a solid foundation the transmission of ENSO signal to rainfall over SESA by determining whether and in what seasons the teleconnection involves VOSA. The full schematic chain of elements is: ENSO→PSA1→VOSA→ rainfall, where the latter linkage is examined in Zamboni et al. (2010).

Building off the results of Zamboni et al. (2010), we stratify the analysis by season in the context of interannual variability. In particular, we include spring and fall, which have been considered by only few authors (Cai and Watterson 2002; Garreaud and Battisti 1999; Robertson and Mechoso 2003; Cazes-Boezio et al. 2003). We start by finding the link between PSA1 and VOSA and their relationships with SST anomalies, particularly with ENSO. This part of the work is based on the National Centers for Environmental Prediction-National Center for Atmospheric Research (NCEP-NCAR) reanalysis. Next, we provide a mechanistic support of our findings with reanalysis data by using the International Centre for Theoretical Physics Atmospheric General Circulation Model (ICTP AGCM) (previously named SPEEDY, Molteni 2003). This part of the work analyzes simulations performed with observed and climatological SSTs in order to separate the internal and forced components of VOSA and PSA1.

The paper is organized as follows. Section 2 describes the datasets we use. Section 3 examines the relationship between PSA1, VOSA and SSTs based on reanalysis data for each season. Section 4 introduces our methodology for separating the internal and forced variability of the atmosphere with the selected AGCM, and the results obtained. Section 5 includes a summary of our findings.

2 Datasets

The present study concentrates on the interannual variability of seasonal circulation over SA and the southern Pacific during the southern spring, summer, and fall seasons. The seasonal mean circulation is represented by the average of the central two-month periods in each season for the period 1948–2002: October–November (ON), January–February (JF), and April–May (AM). The average helps capturing the coherent signal throughout each season while filtering high frequency variability.

The zonal and meridional 200hPa wind, from which the streamfunction is computed, correspond to the global NCEP-NCAR reanalysis. This dataset is available at 2.5° × 2.5° horizontal resolution (Kalnay et al. 1996). The reliability of the early years of the reanalysis (1948–1959), when neither satellite nor radiosonde information were available over South America, is discussed in Sect. 3. We anticipate the data are reliable at the timescale we consider.

For SSTs we use the National Oceanic and Atmospheric Administration's (NOAA) extended reconstructed SSTs dataset (Smith and Reynolds 2004). In this dataset, monthly mean values are available for the global ocean at 2° × 2° horizontal resolution.

The model we use is the intermediate complexity ICTP AGCM (Molteni 2003). The AGCM is configured with 8 vertical (sigma) levels and with a spectral truncation at total wavenumber T30. This AGCM includes physically based parameterizations of large-scale condensation, shallow and deep convection, short-wave and long-wave radiation, surface fluxes of momentum, heat and moisture, and vertical diffusion. Kucharski et al. (2006a) give a more extensive description of the current model version. The selected AGCM has been used in studies of ENSO influences on climate variability in Herzeg-Bulic and Brancovic (2007), Bracco et al. (2004) and Yadav et al. (2010), in investigations of the African and Indian monsoons in Kucharski et al. (2006b, 2009 and 2010), and in research on the South American Monsoon (Barreiro and Tippmann 2008).

Using the ICTP AGCM we performed a 130-year control simulation using climatological, monthly-varying SSTs (i.e. without interannual variations). We will refer to this simulation as CLIMSST. Next we carried out a 35-member ensemble of runs in which the prescribed SSTs correspond to the observation for 1950–2002. Initial conditions of ensemble members differ in small random perturbations. We will refer to the ensemble as ENSM.

3 The relationship between PSA1 and VOSA

As discussed in Zamboni et al. (2010), the EOF patterns of the 200 hPa horizontal winds characterized by VOSA include a cyclonic center on the southwestern side of the EOF domain, corresponding to the far southern part of SA and the surrounding oceans. The result of the EOF analysis are robust when only the data for the period 1959–2002 are considered: in the two cases the explained variance of the

modes differs by few percents and the EOF patterns of interest are very similar. Finally, the correlation between corresponding PCs, on the overlapping period, is 0.99, 0.95, and 0.98 for ON, JF and AM respectively. A second comparison with the ERA40 reanalysis is reported in Zamboni et al. (2010), where the robustness of the results is confirmed. The circulation we described resembles the eastern portion of the PSA1. To obtain a qualitative assessment of the plausibility that VOSA is an integral component of the PSA1 pattern, we regress PCs of VOSA on upper level winds over the Southern Pacific Ocean (Fig. 1). The result for spring clearly shows a wave-like pattern arching from the western Pacific toward high latitudes in the SH and ending over SA. The locations of the associated circulation centers over the South Pacific approximately coincide with those of PSA1 (Mo and Paegle 2001). During the summer, the regression does not capture a PSA1-like feature in the South Pacific and produces a visible result only in proximity of the SA continent

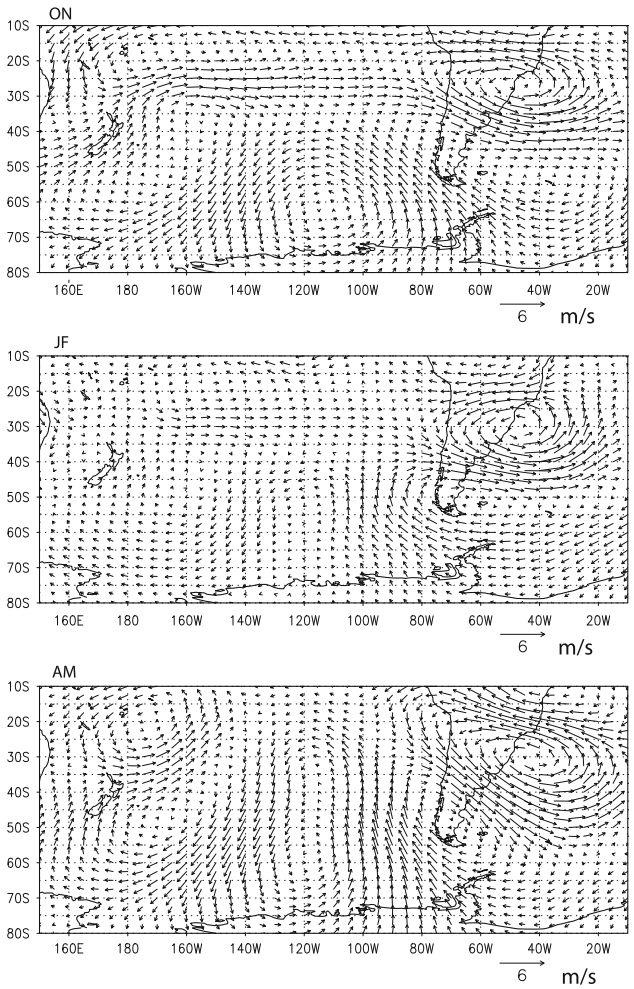

Fig. 1 Regression of PC corresponding to VOSA onto 200 hPa winds over the Pacific Ocean for ON (*upper panel*), JF (*middle panel*), AM (*bottom panel*)

(east of 100W). In the fall, the regression produces a striking wave-like pattern that resembles the one obtained for spring. Although circulation centers are stretched toward the center of the arch they form on the Pacific Ocean, the pattern is strongly similar to PSA1. The circulation obtained by the regression depicts a remarkable seasonality and motivates us to continue our analysis to identify whether VOSA is part of PSA1.

To examine the circulations over the southern Pacific and over SA separately, we perform an EOF analysis of the 200 hPa streamfunction for ON, JF, and AM over two regions in the Southern Hemisphere. The first and larger region extends from 120E to 10E and from the equator to 80S. We will refer to this region, which comprises the Pacific and Atlantic Oceans as well as the part of SA in the Southern Hemisphere, as the Pacific-Atlantic domain. The second region is a sub domain of the former extending over the same range of latitudes but only from 120E to 90W. We will refer to this region as the Pacific domain. For the EOF analysis we neither pre-process nor filter the data, except for working with bimonthly means. We start by comparing the EOF modes corresponding to the two domains and discuss whether and in what season they capture a PSA1 structure. Next, we attempt to connect PSA1 and VOSA. We consider that the connection is established when the results over SA are very similar in pattern and corresponding PCs are highly correlated.

3.1 October–November

Figure 2 displays the variance explained by the EOF modes corresponding to the two domains for ON. In both cases, slopes of the explained variance curve change markedly after the 5th mode, indicating that higher order modes are not discernible from noise. In addition, the variability associated to the 4th and 5th modes is less than 10% of the total. Therefore, the remainder panels in Fig. 2 concentrate on the first three EOFs. These are highly and positively correlated, and substantially present the same patterns over the common domain (see Table 1). There are slight differences in the fraction of variance they explain, particularly for EOF1 (26 and 30% in the large and small domain, respectively) and EOF3 (14 and 16% in the large and small domain, respectively).

We note that retaining the zonal mean produces patterns elongated in the zonal direction compared to those reported in the literature (see also Fig. 1 by Mo and Paegle 2001). An inspection of the patterns shown in Fig. 2 reveals that over the Pacific both EOF1 and EOF3 resemble PSA1. Those EOFs, however, have important differences. The eddy observed over southern SA in EOF1 (60W) results displaced to the east (30W) in EOF3. Further, EOF3 includes a well-defined vortex over the central Pacific

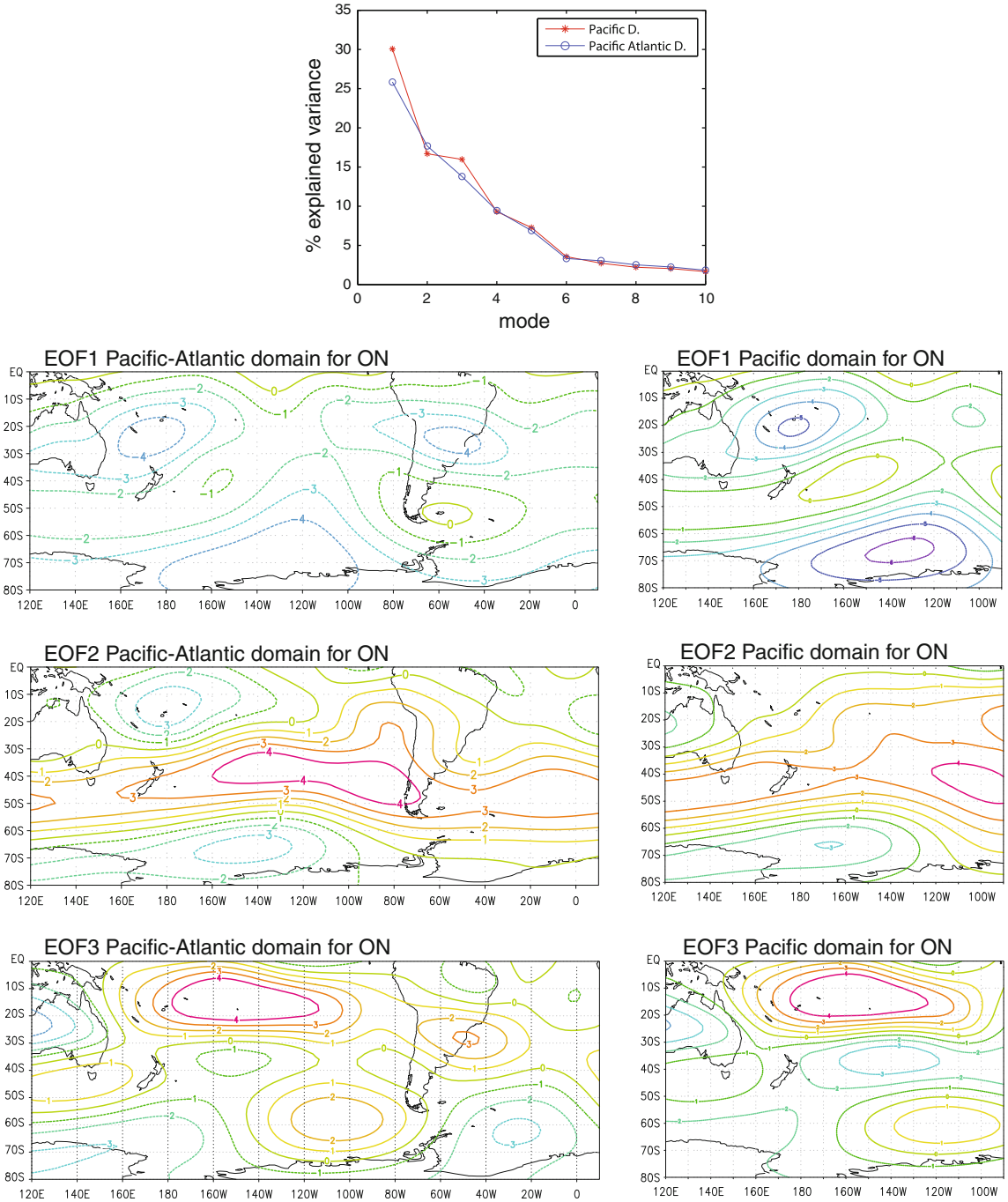

Fig. 2 Comparison between EOF analysis of 200 hPa streamfunction (10^6 m^2/s) for the Pacific and Pacific-Atlantic domains for ON. *Upper panel* is the variance accounted by each mode for the Pacific (*red*) and Pacific-Atlantic (*blue*) domain; *bottom panels* are EOF1, EOF2 and EOF3 for the Pacific-Atlantic domain (*left*), and Pacific domain (*right*)

Table 1 Correlation between PCs obtained in the Pacific and Pacific-Atlantic domains

	PC1	PC2	PC3
ON	0.92	0.78	0.82
JF	0.99	0.96	–
AM	0.97	0.96	0.93

south of the equator, which is not present in EOF1. The latter feature in EOF3 resembles circulation anomalies typical of El Niño years, during which two anticyclones straddling the equator develop over the central-eastern equatorial Pacific with the one south of the equator stretching southeastward toward South America (Rasmusson and Mo 1993). Consistently, PC3 is highly correlated

with the SST anomalies in the tropical Pacific, whereas PC1 is not (see Fig. 3a, b). The PC corresponding to VOSA is only weakly correlated with the SST anomalies in the tropical Pacific (Fig. 3c).

These results suggest that two leading modes (first and third) in the interannual variability in the Southern Hemisphere have patterns resembling PSA1 in the mid-latitudes, and we posit that one of these modes (EOF1) is internally generated by the atmosphere whereas the other (EOF3) is associated with ENSO. Since reanalysis data do not allow us to separate the internal and forced atmospheric variability, in Sect. 4 we carry on this investigation with the ICTP AGCM.

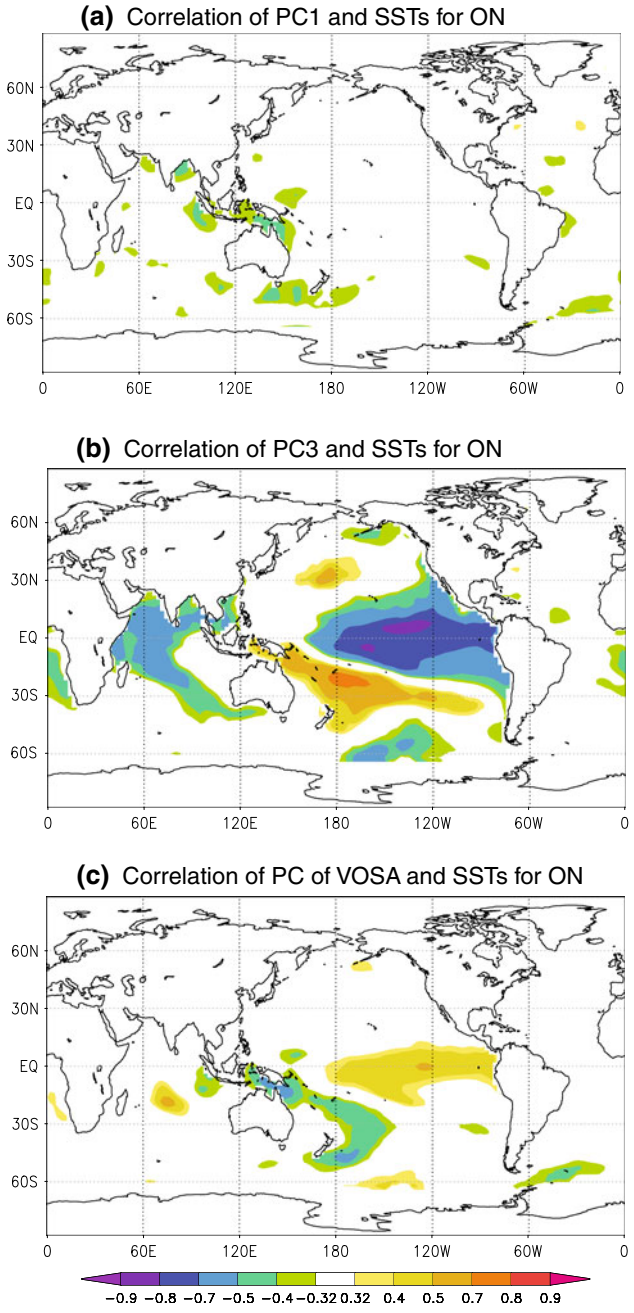

Fig. 3 Correlation map of **a** PC1, **b** PC3 of the Pacific Atlantic domain, and **c** PC of VOSAwith global SSTs for ON. *Shaded areas* are significant at the 95% confidence level

Over SA, both EOF1 and EOF3 for the Pacific-Atlantic domain show features that resemble VOSA. Figure 4 narrows down on the SA domain and superimposes VOSA winds on streamlines of EOF1 (left panel) and EOF3 (right panel) corresponding to the Pacific-Atlantic domain. In each panel the two vortices in the EOFs (winds and streamlines) are centered at almost the same location and extend over the same area. There are also circulations in the opposite directions to the south over the Malvinas islands. The lack of a perfect coincidence between patterns, as revealed in regions where wind vectors cross streamlines, is not an important concern for this study.

To further support the interpretation that VOSA is the part of EOF1 and EOF3 of the Pacific-Atlantic domain, we reconstruct the PC corresponding to VOSA as linear combination of PC1 and PC3 of the Pacific-Atlantic domain as

$$P^{rec} = \frac{\alpha_{11} P_1^p + \alpha_{13} P_3^p}{\sqrt{\alpha_{11}^2 + \alpha_{13}^2}} \quad (1)$$

where P^{rec} is the reconstructed PC of VOSA, P_1^p (P_3^p) is PC1 (PC3) for the Pacific-Atlantic domain, α_{11} is the correlation between PC of VOSA and P_1^p, α_{13} is the correlation between PC of VOSA and P_3^p. The reconstructed timeserie closely follows the original one (Fig. 5), with a correlation of 0.8 (Table 2).

3.2 January–February

The EOF analysis of 200 hPa streamfunction of January-February produces two significant modes, which explain a comparable fraction of the variance in the Pacific and Pacific-Atlantic domains (Table 1). The leading mode presents zonally elongated structures and a circulation center over the central south tropical Pacific (at 140W) with associated anomalous upper level westerlies (Fig. 6). This is the typical structure found over tropical regions during ENSO events, as it is confirmed by the high correlation between the PC and SST anomalies (Fig. 7a). Here we note that the phase depicted by the EOF pattern is associated with La Niña. The second mode represents variations in the intensity of the jet stream at mid-latitudes, and is negatively correlated with SST anomalies in the equatorial Indian Ocean (Fig. 7b). It is apparent that none of the leading modes features a PSA1-like structure in the South Pacific. According to the reanalysis data, therefore, in January and February VOSA is unrelated to the circulation over the Pacific. These results emphasize the existence of significant seasonal differences in the Southern Hemisphere circulation, and that the PSA modes are less relevant in the summer season.

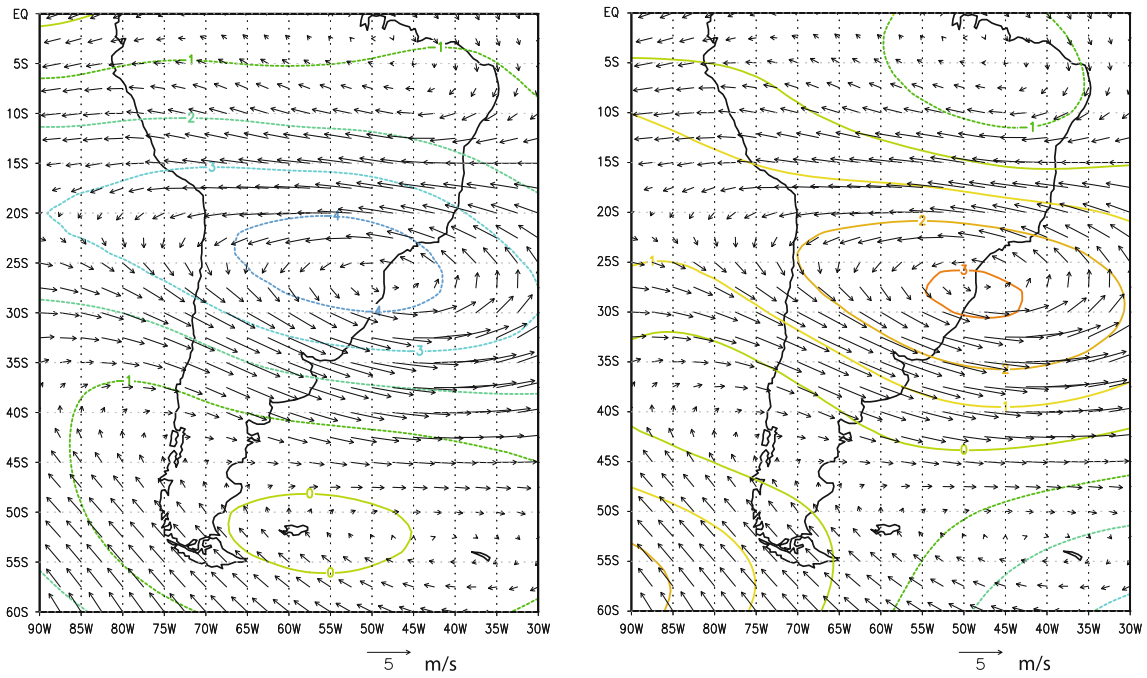

Fig. 4 Comparison between VOSA (vectors, m/s) and Pacific-Atlantic domain EOF1 (*left*, contours in 10^6 m^2/s) and EOF3 (*right*, contours in 10^6 m^2/s)

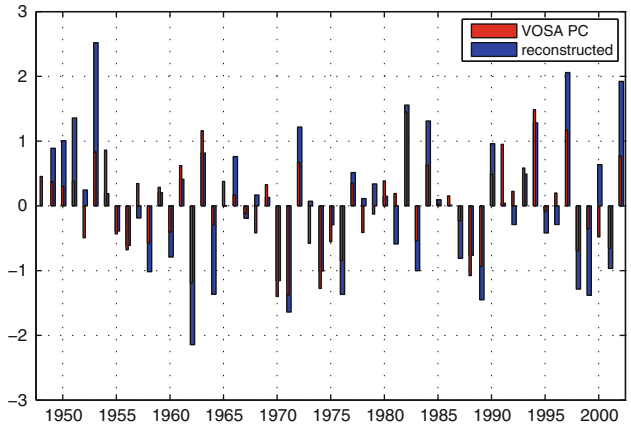

Fig. 5 Reconstructed PC of VOSA (*blue*) and PC of VOSA (*red*) for ON

Table 2 Correlation of PC of VOSA with PC1 and PC3 of the Pacific and Pacific-Atlantic domains, and the reconstruction of the former (see text for details)

	PC1	PC3	P_1^p
ON	0.55	−0.57	0.8
AM	0.63	−0.56	0.85

An attempt to directly relate VOSA with SSTs shows small but statistically significant correlations over the Indian Ocean (Fig. 7c). We are not aware of reported teleconnections between the two regions that do not involve either the PSA modes or ENSO. Performing an additional experiment in which observed SSTs are set over the Indian Ocean while climatological SSTs are imposed elsewhere, might elucidate this point. However, since the relationship between PSA1 and VOSA, which is our focus, is not found in JF, this problem is beyond the scope of the present investigation. As local mechanisms during the monsoon season over SA appear to dominate over remote teleconnections (Grimm 2003; Grimm et al. 2007), our intuition is that the correlation we see between VOSA and SSTs in the Indian Ocean at the interannual timescale are not indicative of a dynamical link between the two regions.

3.3 April–May

In this season, the EOF analysis of 200 hPa streamfunction produces three significant modes. Corresponding patterns for the Pacific-Atlantic and Pacific domains are practically identical (not shown) and their corresponding PCs are highly correlated (Table 1). As for spring, both EOF1 and EOF3 present over SA a circulation pattern resembling VOSA, and for this reason we focus the analysis on these two modes (Fig. 8). EOF1 is characterized by a zonal flow in which alternate centers of anomalies are embedded and particularly pronounced over SA. The lack of a well-defined closed circulation over high latitudes (60–70S) at 120W makes the identification of EOF1 as PSA1 uncertain, while the pattern over Australia and over SA would support such identification.

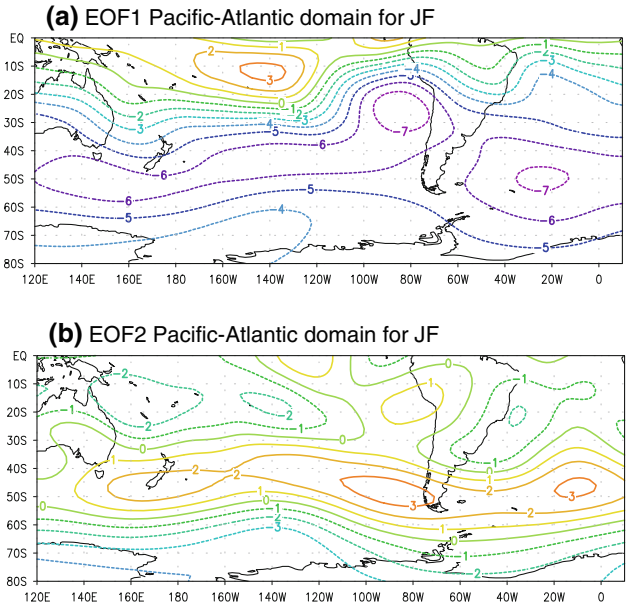

Fig. 6 **a** EOF1 and **b** EOF2 of the 200 hPa streamfunction (10^6 m^2/s) over the Pacific-Atlantic domain for JF

The correlation between the corresponding PC and SSTs is barely significant (0.4–0.5) over the western tropical Atlantic, central tropical Pacific and northeastern Indian Ocean (Fig. 9a), thus EOF1 is likely to be a mode of internal variability. The 3rd leading pattern resembles PSA1: the concave arch depicted by the anomalous centers is clearly visible and spans the whole southern Pacific. The correlation of PC3 and SSTs over the Pacific shows a clear ENSO signature. There are negative values over the Indian Ocean and over the western subtropical Atlantic on the South American coast (Fig. 9 b) as large as those over the equatorial Pacific. The distribution in Fig. 9 is almost identical to the correlation map between PSA1 and global SSTs obtained by Mo and Paegle (2001). These results suggest that ENSO is the primary forcing of the observed pattern, which induces SST anomalies in the Indian Ocean, while internal atmospheric variability induces those close to the South American coast and at 160W, 60S (Zamboni et al. 2010).

Over SA, EOF1 and VOSA (Fig. 10 left panel) are markedly similar: they present a well-defined eddy over the continent and a circulation in the opposite direction to the south. The correlation between corresponding PCs is 0.63 (Table 2). Roughly similar considerations to the previous case hold for the comparison between EOF3 and VOSA (Fig.10 right panel), in particular vortices depicted by the two variables are stretched along the northwest-southeast direction and present opposite circulation to the south except for slight displacements in the centers of anomalies. The correlation between corresponding PCs is −0.56.

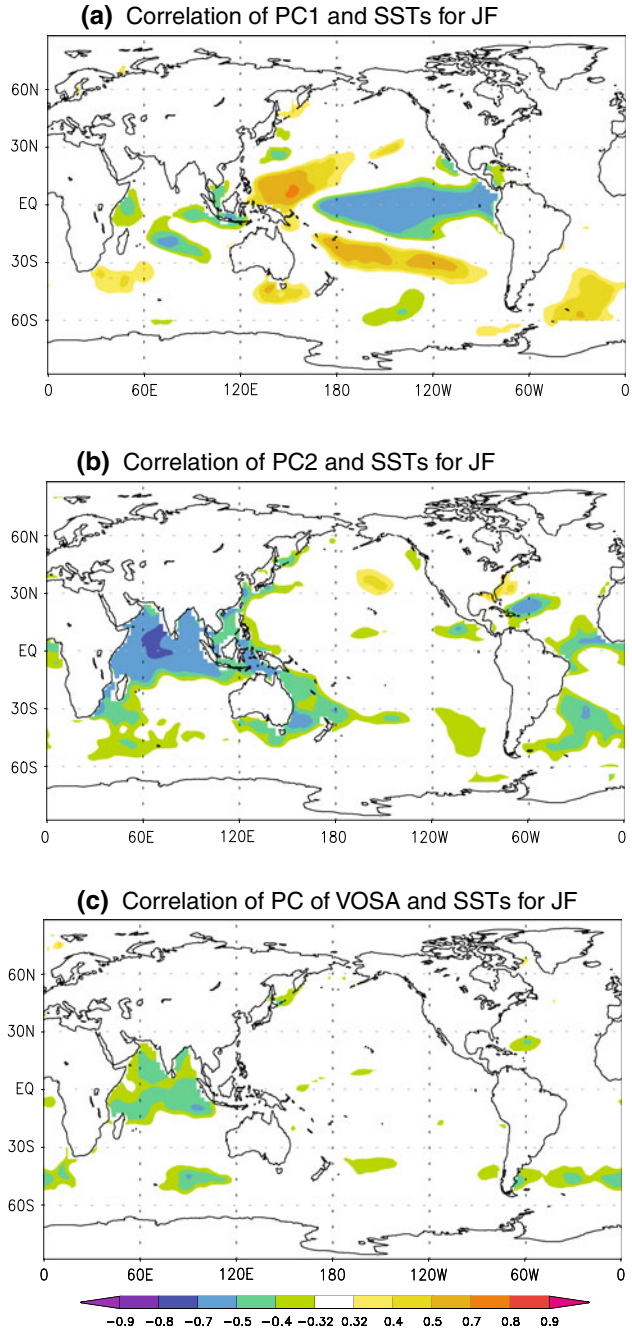

Fig. 7 Correlation map of **a** PC1, **b** PC2 of the Pacific Atlantic domain, and **c** PC of VOSA with global SSTs for JF. *Shaded areas* are significant at the 95% confidence level

4 AGCM experiments

In order to separate the internal and forced variability and support our interpretation of results with reanalysis data, we performed numerical experiments with the ICTP AGCM. Our control simulation is a 130-year long run using climatological, monthly-varying SSTs (i.e. without interannual variations). We will refer to this simulation as

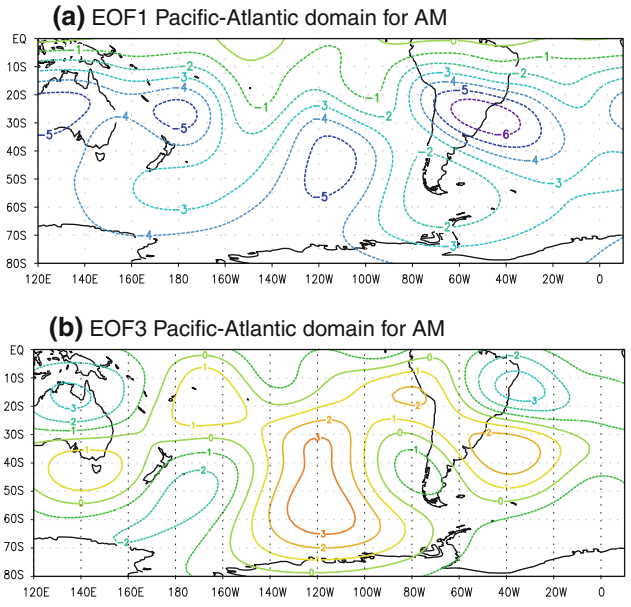

Fig. 8 EOF analysis of 200 hPa streamfunction (10^6 m^2/s) for Pacific-Atlantic domain for AM. **a** EOF1, **b** EOF3

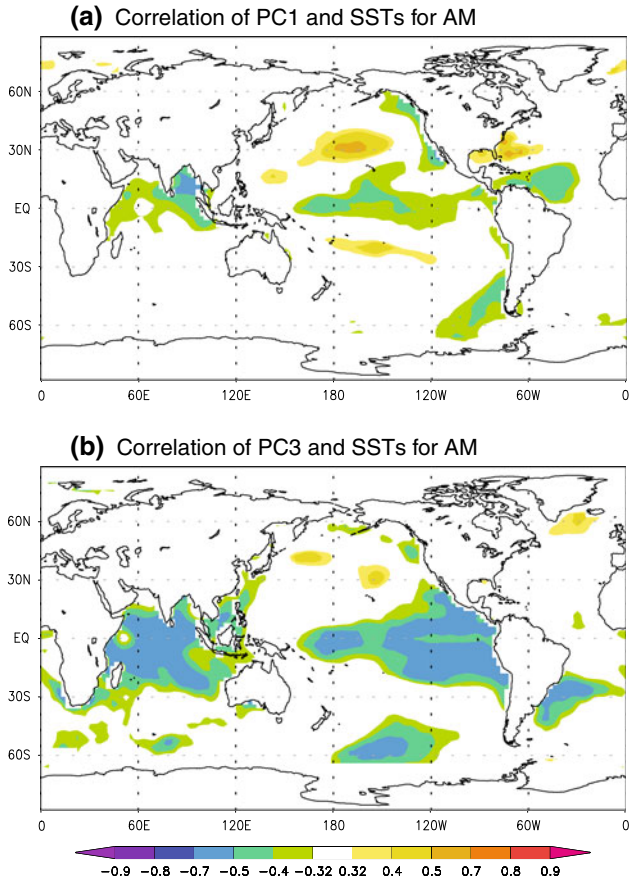

Fig. 9 Correlation map of **a** PC1 and **b** PC3 of 200 hPa streamfunction of the Pacific-Atlantic domain with SSTs for AM. *Shaded areas* are significant at the 95% confidence level

CLIMSST. Next we carried out a 35-member ensemble of runs in which the prescribed SSTs correspond to the observation for 1950–2002. Initial conditions of ensemble members differ in small random perturbations. We will refer to the ensemble as ENSM.

The EOF analysis of the covariance matrix of the 200 hPa streamfunction of CLIMSST and ENSM produce the model internal and forced modes of variability respectively (Straus and Shukla 2000). The domain of the EOF analysis is from 90W to the prime meridian, and from the equator to 60S. (Black box in Figs. 12, 13 and 14). Forced modes obtained with the procedure we are applying may depend on the ensemble, especially if the system is characterized by a small signal/noise ratio. To add confidence to the analysis, we compare the internal variability in CLIMSST and ENSM. The latter is obtained by subtracting the ensemble mean from each member first and performing the EOF analysis on the remainder fields. The internal modes obtained by the two methodologies compare remarkably well for all seasons (not shown).

In this section our objective is to identify internal and forced patterns that comprise either a vortex similar to VOSA or the leading PSA; all other modes of the ICTP AGCM are not discussed.

4.1 ON AGCM

Figure 12 presents the regression of the first three PCs of internal variability of streamfunction (left panels), obtained for the region highlighted by black box in the figures, onto the same field over the globe. The leading mode (Fig. 12a) has an evident zonal structure, but presents a local vortex over SA similar to VOSA. The 2nd (Fig. 12b) and 3rd (Fig. 12c) modes clearly depict wave-like patterns over the SH with larger amplitude over the SA sector. We notice in particular that EOF3 has a PSA1-like feature in the South Pacific in addition to a vortex over SA, which compares with VOSA very well. A quantitative association of the internal modes with VOSA, as it would be given for example by the correlation between corresponding PCs, cannot be made. In fact the PCs of the internal modes do not represent a temporal series but rather the amplitude of the modes in the sequence of members of the ensemble. Instead, the correspondence with time of the forced mode exists since all members share the same forcing each year, and the ensemble mean is its expression.

The only forced pattern of interest to our specific objectives is that of EOF3 (Fig. 12d). This pattern consists of an anticyclonic pair straddling the equator and alternate centers of anomalies over the Southern Hemisphere arching poleward before being refracted equatorward over the SA continent and Atlantic Ocean. To the north, the PNA pattern can also be identified. Compared to the results

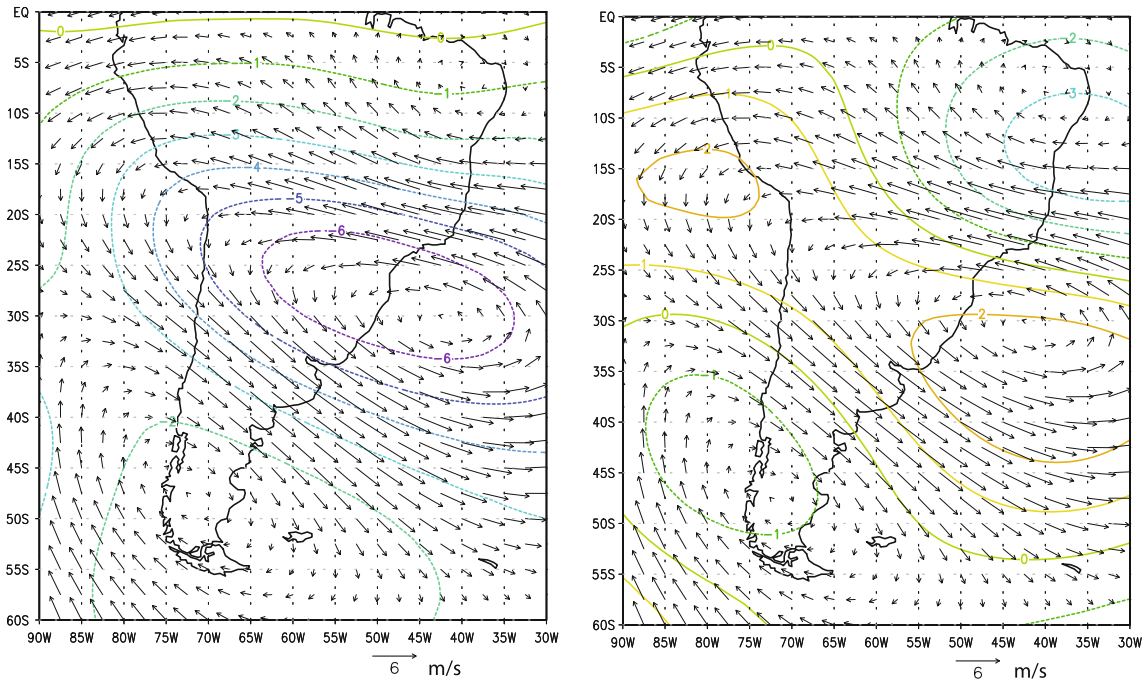

Fig. 10 Patterns comparison of VOSA (vectors, m^2/s) and Pacific-Atlantic domain EOF1 (*left*, contours in 10^6 m^2/s) and EOF3 (*right*, contours in 10^6 m^2/s) for AM

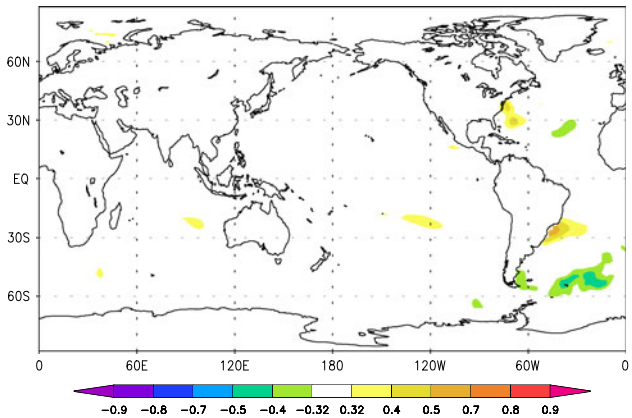

Fig. 11 Correlation map of PC of VOSA onto simultaneous SSTs for AM. *Shaded areas* are significant at the 95% confidence level

obtained with reanalysis data, the simulation exaggerates the anticyclones over the tropics, which in turn shrink the pattern of interest to the south and to the west especially over SA. Nonetheless, the pattern can be interpreted as PSA1, and it is related to ENSO (Fig. 12e).

The extent to which VOSA is the expression of internal versus forced variability is quantified by the ratio between the variance of the latter and the total (Bracco et al. 2004). As expected, the ratio decreases with latitude from the tropics to higher latitudes and has minimum values in the region of VOSA (Fig. 12f), which is due to increased noise at those locations (not shown). The lack of a pattern of minima in the proximity of PSA1 circulation centers supports the idea that VOSA can also be an expression of continental scale internal variability not related to the PSA1. This conclusion is consistent with EOF1 of internal variability (Fig. 12a), which, as discussed, presents an isolated vortex over SA and it is not accompanied by a comparable forced mode.

On the ground of these results, we conclude that VOSA is mainly part of the PSA1 pattern, which is primarily expression of atmospheric internal variability but also ENSO-related forced variability. The simulation with the ICTP AGCM further suggests that VOSA can also be expression of *local* internal variability.

4.2 JF AGCM

The EOF1 of the internal variability in JF is very similar to that in ON, except that the flow is more zonal (Fig. 13a). EOF3 of the internal component (Fig. 13b) consists of a zonal structure at high latitude and alternating centers of anomalies over the Pacific at subtropical latitudes. Such a pattern can be interpreted as a combination of PSA1 and the high-latitude mode (Kidson 1988). Over SA, the pattern consists of a vortex circulation similar to VOSA, and of a second vortex to the south. EOF3 is the only pattern of interest of the forced variability; it comprises an isolated upper level cyclonic circulation that resembles VOSA (Fig. 13c), even though it is slightly displaced over the ocean, and a circulation in the opposite direction to the south. Such vortex has a baroclinic structure (Fig. 13d),

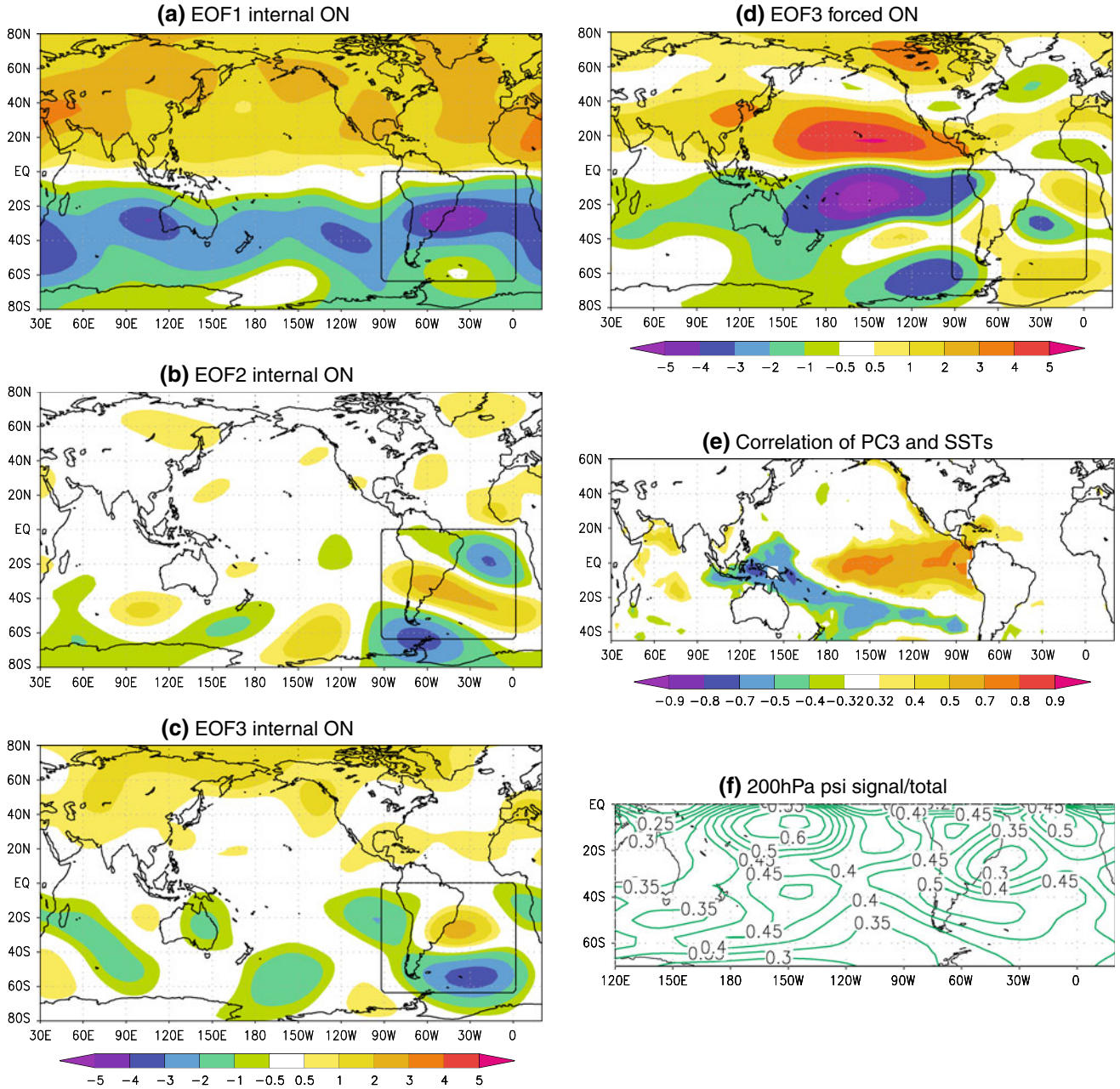

Fig. 12 ICTP AGCM for ON. Regression of **a** PC1, **b** PC2, **c** PC3 of the internal variability, and **d** PC3 of the forced variability of 200 hPa streamfunction (10^6 m^2/s) onto the same field over the globe. The *black box* indicates the domain of the EOF analysis. **e** is the correlation of PC3 of the forced variability with SSTs, **f** is the signal-to-total-ratio

which distinguishes it from VOSA (Zamboni et al. 2010). The structure is consistent with the oceanic forcing suggested by the correlation of the corresponding PC and global SSTs (Fig. 13e). A further investigation of this circulation is beyond the scope of the present study.

We underline that PSA1 appears only as the third mode of internal variability in combination with the high-latitude mode, supporting the idea that in the summer it is not a relevant mode as it is in other seasons. The circulation over SA is primarily unrelated to that over the southern Pacific, in agreement with Grimm (2003), but, similarly to other seasons, it is characterized by a continental scale vortex at subtropical latitudes, which is expression of both the internal and forced variability by Atlantic SSTs anomalies.

4.3 AM AGCM

The 2nd mode of internal variability in April-May has a wave-like pattern with larger amplitudes over the Southern Pacific sector similar to PSA1, and also a vortex over SA

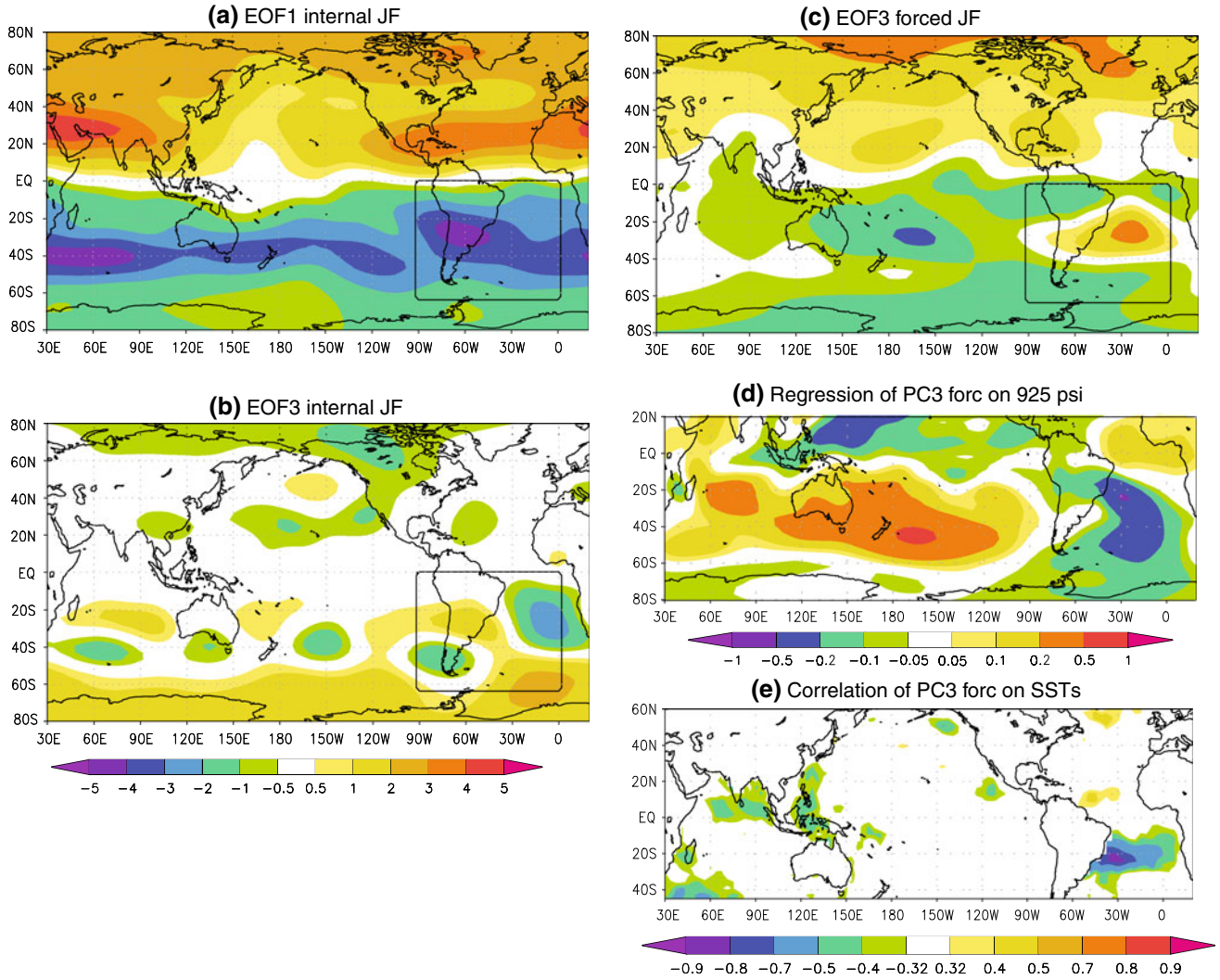

Fig. 13 ICTP AGCM for JF. Regression of **a** PC1 and **b** PC3 of the internal variability of 200 hPa streamfunction (10^6 m^2/s). **c** same as **b** but for the forced component, **d** is the regression of PC3 onto 925 hPa streamfunction (10^6 m^2/s), **e** correlation of PC3 with global SSTs

resembling VOSA (Fig. 14a). In contrast to the analysis based on observations, none of the forced modes in the ICTP AGCM presents the PSA1 pattern. This signal is possibly too small to be reproduced by the model. The only forced pattern of interest is EOF3. It presents a localized vortex comparable to VOSA and opposite circulation to the south (Fig. 14b). Similarly to the summer, the vortex has a baroclinic structure (Fig. 14c) consistent with the impact of SST anomalies in the Atlantic (Fig. 14d).

We stress that during both JF and AM upper level continental scale vortices can be part of an equivalent barotropic structure, which induces SST anomalies in the underlying ocean (Zamboni et al. 2010, Robertson and Mechoso 2000), but can also be part of a baroclinic structure forced by SSTa. Even though the SST pattern of the latter is located to the north compared to the former, we underline the importance of the presence of both structures because of the potential implications for predictability over SA.

5 Summary and discussion

Building on recent findings by Zamboni et al. (2010), we explored the relationship between a barotropic continental scale vortex over SA (VOSA) and the leading PSA mode of interannual variability in the Southern Hemisphere (PSA1). The investigation is motivated by the relevance of VOSA in impacting seasonal precipitation via modulation of the SALLJ and flow from subtropical Atlantic in October-November (ON), January–February (JF), and April–May (AM), and consequent implications for seasonal forecasts.

We searched for relationships between the circulation over the Southern Pacific and continental South America

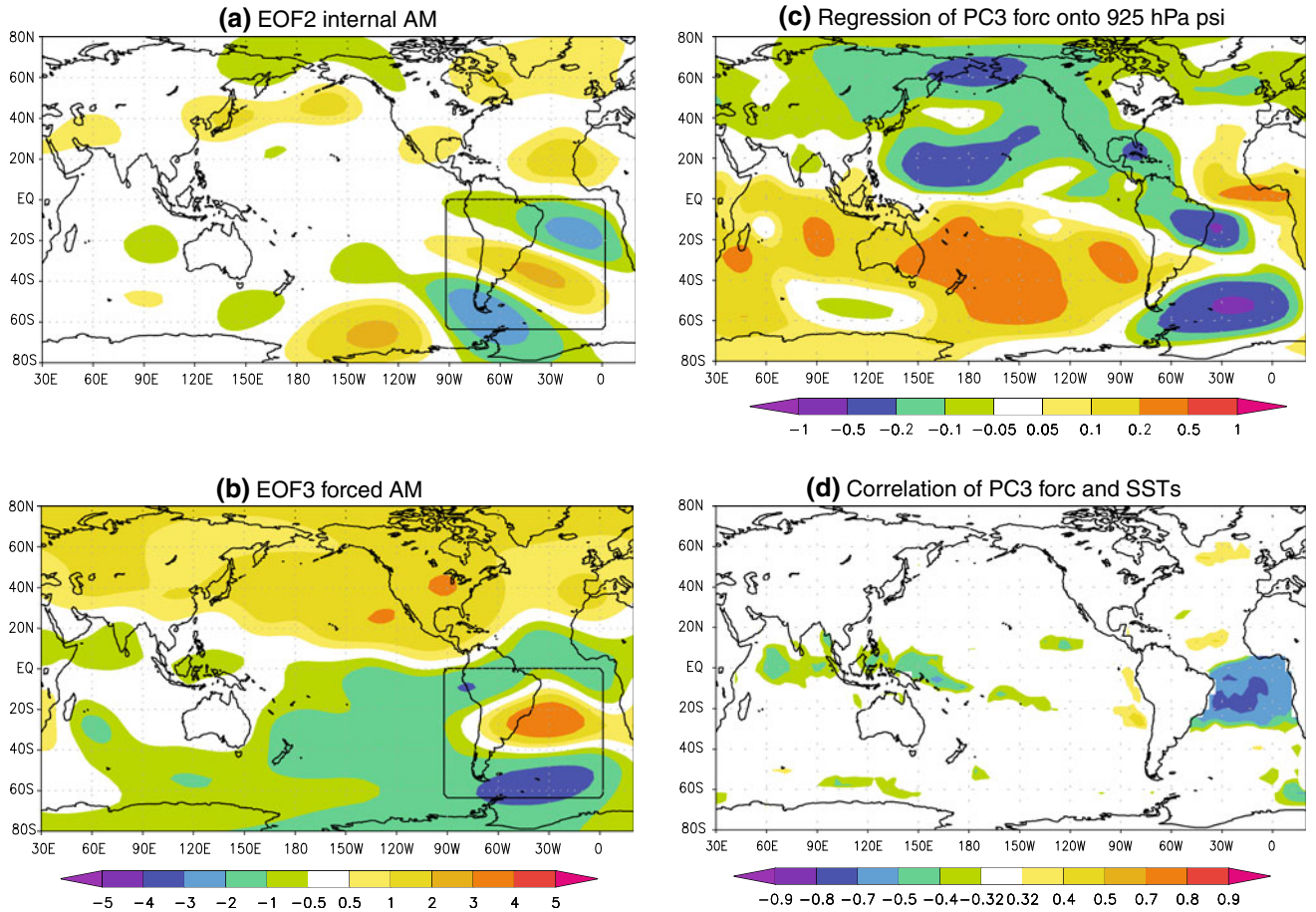

Fig. 14 ICTP AGCM for AM. Regression of **a** PC2 of the internal variability, **b** PC3 of the forced variability of 200 hPa streamfunction (10^6 m^2/s) onto the same field over the globe. **c** regression of PC3 of forced variability onto 925 hPa streamfunction (10^6 m^2/s), **d** correlation of PC3 of forced variability with global SSTs

with the aim of determining whether VOSA is an integral part of PSA1 or whether these two important features of the interannual variability are primarily independent of each other. The methodology used is mainly based on reanalysis data (see Sect. 3) for the period 1948–2002. We also performed numerical integrations with the ICTP AGCM in order to obtain a better understanding of the separation between the internal and forced variability of the SH (see Sect. 4) We have investigated each season of interest individually, which has previously been done by only few authors, especially for the spring and fall (Cai and Watterson 2002; Garreaud and Battisti 1999; Robertson and Mechoso 2003; Cazes-Boezio et al. 2003).

According to our results, in spring PSA1 is the result of both internal and forced variability, the latter being forced by ENSO (Figs. 2, 3). The forced component appears as frequently as half of the occurrences of the corresponding internal mode, consistently with the larger relevance of ENSO in this season. VOSA appears primarily in association with PSA1, but can also be the expression of *local* internal variability, as suggested by the simulation (Fig. 12). Such a dual character reduces VOSA predictability compared to that of PSA1. In view of the high similarity of the vortices over SA, the EOF analysis does not discriminate between the internal and forced components when the domain coincides with the continental SA (Zamboni et al. 2010). The two components separate when the domain of the EOF computation includes the Pacific and Atlantic Oceans. This is due to significant differences, particularly evident over the Tropical Pacific, between the internal and forced patterns in which VOSA is embedded.

The summer season presents the largest departure with respect to the occurrence of PSA obtained by pooling all seasons together (as for example found in Mo and Paegle 2001). The PSA mode is not a dominant circulation: it is not revealed in the reanalysis data and appears only as mixed to the high-latitude mode in the ICTP AGCM (Fig. 13b). In searching for low frequency signals to the interannual variability Barreiro (2009) identified a different modulation of Atlantic SSTs to the climate over subtropical SA. In JF and late spring Andreoli and Kayano (2005) observed different circulation patterns over the SH and

precipitation anomalies over SA, for the periods before and after the mid-'70s, which correspond to different phases of the Pacific Decadal Oscillation. Similarly to our results, PSA1 was not found in neither case during JF in their study. As precipitation anomalies associated with VOSA over SA are remarkably similar in different seasons (Zamboni et al. 2010), while the upper level circulation over the southern Pacific in summer is significantly different compared to spring and fall, our intuition is that in summer VOSA is an expression of internal (Fig. 7c) local continental scale circulation over SA (Figs. 6, 13).

In the southern fall, VOSA is mainly expression of internal atmospheric variability related to PSA1, even though the identification of PSA1 as internal mode in the reanalysis is less firm in this season (Fig. 8a). A contribution of the forced variability to VOSA and PSA1 is found in the reanalysis (Fig. 8b); however, it accounts for a much smaller fraction of the variance compared to that of the internal component. Possibly for this reason, the forced PSA1 is not reproduced by the simulation. These results are all consistent with a better capability of state of the art GCMs in reproducing VOSA in the spring than for the other seasons (Zamboni et al. 2010).

The physical processes underlying the establishment of VOSA remain an open question after this study. We expect VOSA to be related to intrinsic features of the South American continent such as its orography, since it is a dominant circulation in all the seasons we investigated. The dominant role of the regional circulation associated with the South American Monsoon (Grimm 2003; Grimm et al. 2007) in summer further suggests that interactions of the atmosphere with land-surface conditions could contribute in this season in generating VOSA. Investigations with a coupled atmospheric-land-surface GCM (or a regional model) may shade light on this aspect.

Finally, it would be of further value to explore the potential predictability of VOSA and thus precipitation further by for example investigating its relationship with low frequency variability, as different phases of decadal variability could be mixed in the 50 years we analyzed.

Acknowledgments This research was supported by NOAA under grant NA05OAR4310009 and by the Abdus Salam International Centre for Theoretical Physics.

References

Aceituno P (1988) On the functioning of the Southern Oscillation in the South American sector. Part I Surface Clim Mon Wea Rev 116:505–524

Andreoli RV, Kayano MT (2005) ENSO-related rainfall anomalies in South America and associated circulation features during warm and cold Pacific decadal oscillation regimes. Int J Climatol 25:2017–2030. doi:10.1002/joc.1222

Barreiro M, Tippmann A (2008) Atlantic modulation of El Niño influence on summertime rainfall over southeastern South America. Geophys Res Lett 35:L16704. doi:10.1029/2008GL035019

Barreiro M (2009) Influence of ENSO and the south Atlantic ocean on climate predictability over Southeastern South America. Clim Dyn 35:1493–1508. doi:10.1007/s00382-009-0666-9

Bracco A, Kucharski F, Kallummal R, Molteni F (2004) Internal variability, external forcing and climate trends in multi-decadal AGCM ensembles. Clim Dyn 23:659–678

Cai W, Watterson IG (2002) Modes of interannual variability of the Southern Hemisphere circulation simulated by the CSIRO climate model. J Clim 15:1159–1174

Carril AF, Navarra A (2001) The interannual leading modes of the extratropical variability in the Southern Hemisphere simulated by the ECHAM-4 atmospheric model. Clim Dyn 18:1–16

Cazes-Boezio G, Robertson AW, Mechoso CR (2003) Seasonal Dependence of ENSO teleconnections over South America and relationships with precipitation over Uruguay. J Clim 16:1159–1176

Diaz A, Aceituno P (2003) Atmospheric circulation anomalies during episodes of enhanced and reduced convective cloudiness over Uruguay. J Clim 16:3171–3185

Garreaud RD, Battisti DS (1999) Interannual (ENSO) and interdecadal (ENSO-like) variability in the Southern Hemisphere tropospheric circulation. J Clim 12:2113–2123

Ghil M, Mo K (1991) Intraseasonal oscillations in the global atmosphere. Part II Southern Hemisphere. J Atmos Sci 48:780–790

Grimm AM, Ferraz SET, Gomes J (1998) Precipitation anomalies in Southern Brazil associated with El Niõ and La Niã events. J Clim 11:2863–2880

Grimm AM, Barros VR, Doyle ME (2000) Climate variability in Southern South America associated with El Niõ and La Niã events. J Clim 13:35–58

Grimm AM (2003) The El Niõ impact on the summer monsoon in Brazil) regional processes versus remote influences. J Clim 16:263–280

Grimm AM, Pal JS, Giorgi F (2007) Connection between spring conditions and peak summer monsoon rainfall in South America role of soil moisture, surface temperature, and topography in Eastern Brazil. J Clim 20:5929–5945

Herceg Bulic I, Brankovic C (2007) ENSO forcing of the Northern Hemisphere climate in a large ensemble of model simulations based on a very long SST record. Clim Dyn 28:231–254

Kalnay E, Kanamitsu M, Kistler R, Collins W, Deaven D, Gandin L, Iredell M, Saha S, White G, Woollen J, Zhu Y, Leetmaa A, Reynolds R, Chelliah M, Ebisuzaki W, Higgins W, Janowiak J, Mo KC, Ropelewski C, Wang J, Jenne R, Joseph D (1996) The NCEP/NCAR 40-year reanalysis project. Bull Amer Meteor Soc 77:437–470

Karoly DJ (1989) Southern Hemisphere circulation features associated with El Niõ-Southern Oscillation events. J Clim 2:1239–1252

Kidson JW (1988) Interannual variations in the Southern Hemisphere circulation. J Clim 1:1177–1198

Kidson JW (1999) Principal Modes of Southern Hemisphere low-frequency variability obtained from NCEP-NCAR reanalyses. J Clim 12:2808–2830

Kiladis GN, Mo KC (1998) Interannual and intraseasonal variability in the Southern Hemisphere. In: Karoly DJ, Vincent D (eds) The meteorology of the Southern Hemisphere. American Meteorological Society, Boston, pp 307–336

Kucharski F, Molteni F, Bracco A (2006) Decadal interactions between the Western Tropical Pacific and the North Atlantic Oscillation. Clim Dyn 26:79–91. doi:10.1007/s00382-005-0085-5

Kucharski F, Molteni F, Yoo JH (2006) SST forcing of decadal Indian monsoon rainfall variability. Geophys Res Lett 33:L03709. doi:10.10029/2005GL025371

Kucharski F, Bracco A, Yoo JH, Tompkins AM, Feudale L, Ruti P, Dell'Aquila A (2009) A Gill-Matsun-type mechanism explains the tropical Atlantic influence on African and Indian monsoon rainfall. Quart J R Met Soc 135:569–579. doi:10.1002/qj.406

Kucharski F, Bracco A, Barimalala R, Yoo JH (2010) Contribution of the east-wets thermal heating contrast to the South Asian Monsoon and consequences for its variability. Clim Dyn. doi:10.1007/s00382-010-0858-3

Lau KM, Sheu PJ, Kang IS (1994) Multiscale low-frequency circulation modes in the global atmosphere. J Atmos Sci 51:1169–1193

Mo KC, Ghil M (1987) Statistics and dynamics of persistent anomalies. J Atmos Sci 44:877–902

Mo KC, Higgins RW (1998) The Pacific-South American modes and tropical convection during the Southern Hemisphere winter. Mon Wea Rev 126:1581–1596

Mo KC (2000) Relationships between low-frequency variability in the Southern Hemisphere and Sea surface temperature anomalies. J Clim 13:3599–3610

Mo KC, Paegle JN (2001) The Pacific-South American modes and their downstream effects. Int J Climatol 21:1211–1229

Molteni F (2003) Atmospheric simulations using a GCM with simplified physical parametrizations. (I) Model climatology and variability in multi-decadal experiments. Clim Dyn 20:175–191

Montecinos A, Diaz A, Aceituno P (2002) Seasonal diagnostic and predictability of rainfall in subtropical South America based on tropical pacific SST. J Clim 13:746–758

Pisciottano GJ, Diaz AF, Cazes-Boezio G, Mechoso CR (1994) El Niõ-Southern Oscillation impact on rainfall in Uruguay. J Clim 7:1286–1302

Rao VB, Hada K (1990) Characteristics of rainfall over Brazil: annual variations and connections with the Southern Oscillation. Theor Appl Climatol 42:81–91

Rasmusson EM, Mo K (1993) Linkages between 200-mb tropical and extratropical circulation anomalies during the 1986–1989 ENSO cycle. J Clim 6:595–616

Robertson AW, Mechoso CR (2000) Interannual and interdecadal variability of the South Atlantic convergence zone. Mon Wea Rev 128:2947–2957

Robertson AW, Mechoso CR (2003) Circulation regimes and low-frequency oscillations in the South Pacific sector. Mon Wea Rev 131:1566–1576

Silvestri GE (2004) El Niõ signal variability in the precipitation over southeastern South America during austral summer. Geophys Res Lett 31:L18206. doi:10.1029/2004GL020590

Smith TM, Reynolds RW (2004) Improved extended reconstruction of SST (1854–1997). J Clim 17:2466–2477

Straus DM, Shukla J (2000) Distinguishing between the SST-forced variability and internal variability in mid latitudes. Analysis of observations and GCm simulations. Q J R Meteorol Soci 126:2323–2350

Yadav RK, Yoo JH, Kucharski F, Abid MA (2010) Why is ENSO influencing Northwest India winter precipitation in recent decades? J Clim 23:1979–1993

Zamboni L, Mechoso CR, Kucharski F (2010) Relationships between upper-level circulation over South America and rainfall over Southeastern South America. A physical base for seasonal predictions. J Clim 23(12):3300–3315

Zhou J, Lau KM (2001) Principal modes of interannual and decadal variability of summer rainfall over South America. Int J Climatol 21:1623–1644